TIME MIGRATION APPLYING THE i-CRS OPERATOR

M. Bobsin, B. Schwarz, C. Vanelle, and D. Gajewski

email: *martina.bobsin@uni-hamburg.de*
keywords: *Time Migration, i-CRS*

ABSTRACT

The aim of applied seismic is to image the subsurface. The data processing required to achieve this goal includes different steps, for example multi-parameter stacking and time migration. The recently-introduced implicit common reflection surface (i-CRS) stacking operator is suitable for reflections as well as for diffractions. In order to further exploit this property, we have developed an i-CRS diffraction summation migration technique for the prestack case. An advantage of the method is that no additional velocity modelling is necessary because the migration velocity is calculated from the kinematic wave field attributes, a prescribed near surface velocity, and the considered zero-offset (ZO) time. The kinematic wave field attributes are available after the i-CRS stacking. i-CRS migration is therefore, a purely data-driven process. In this study, we apply the i-CRS stacking and migration operator to synthetic and field data. In the results, sedimentary layers as well as complex geological features such as diffractors or fault zones are well resolved.

INTRODUCTION

The goal of applied seismic is the imaging of the subsurface. To obtain such an image, a seismic experiment is carried out, which leads to information about subsurface parameters, e.g. density, reservoir thickness, porosity development, and permeability properties. After pre-processing the acquired data, time imaging is performed, which includes stacking and time migration. These two important steps are the topic of this paper.

The classical common midpoint (CMP) stack was introduced by Mayne (1962). He approximates the travel time move out of seismic events, e.g., reflections, by a hyperbola. It is described by the stacking velocity, a parameter determined to provide the best fit of the hyperbolic approximation to the travel times of the events. CMP-stacking is carried out along one direction, namely offset direction. Multi-parameter stacking operators like the common reflection surface (CRS; Müller, 1999), multifocusing (Gelchinsky et al., 1999), and implicit common reflection surface (i-CRS; Vanelle et al., 2010; Schwarz et al., 2014), on the other hand, stack over the midpoint direction as well. The three parameters needed to describe these operators are the so-called kinematic wave field attributes introduced by Hubral (1983), the curvatures of two hypothetical wave fronts and the incidence angle. The higher number of traces involved in multi-parameter stacking leads to an improved signal-to-noise ratio in comparison with the classical CMP stack.

In contrast to stacking, time migration focuses the energy and can provide a corrected geological image of the subsurface. A migration approach known for a long time is summation migration, a special type of Kirchhoff time migration (e.g., Yilmaz, 2001), which considers diffraction travel times described by analytic operators. Accordingly, the amplitudes are summed up along the diffraction travel time and the result is assigned to the apex of the diffraction hyperbola. The main benefit of migration in comparison to stacking are that reflections are dip and length corrected and that diffracted energy is collapsed. However, migration only leads to a focused image if a suitable velocity is used for the calculation of the diffraction travel times. Such a velocity can be obtained, e.g., from an appropriate stacking operator.

In this study, we derive a prestack time migration (PreSTM) operator based on the i-CRS operator (Schwarz
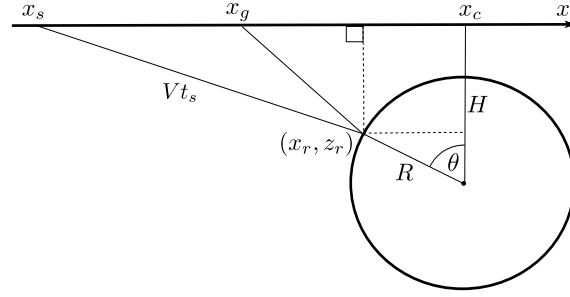
Figure 1: i-CRS geometry (Schwarz, 2011). The circle is described by its centre point (x_c, H) and the radius R. The constant velocity is denoted by V. The angle θ can be determined in an implicit way by evaluating Snell's law (Vanelle et al., 2010).

et al., 2014). The principle of summation migration acts as the basic framework for the operator. We have applied the new method to synthetic and field data to investigate the quality of the images. The obtained images are promising for simple as well as complex geological structures.

THEORY

Vanelle et al. (2010) introduced the i-CRS stacking operator. It is a double square root (DSR) operator based on the assumptions of a homogeneous auxiliary medium and geometrical optics. The approach is model based and considers a circular reflector in the subsurface on which the reflection point $(R \sin \theta, H - R \cos \theta)$ is determined (see Figure 1). The travel time reads as follows:

$$t = t_s + t_g, \tag{1a}$$

$$t_s = \frac{1}{V} \sqrt{(x_m - h - x_c - R \sin \theta)^2 + (H - R \cos \theta)^2}, \tag{1b}$$

$$t_g = \frac{1}{V} \sqrt{(x_m + h - x_c - R \sin \theta)^2 + (H - R \cos \theta)^2}, \tag{1c}$$

where the coordinates x_m and h are the midpoint and half-offset, respectively. The angle θ is determined by an iterative solution of an implicit expression as described by Vanelle et al. (2010). In the next section, we introduce the derivation of an i-CRS migration operator.

Migration operator

In order to derive the i-CRS migration operator, we consider diffractions, where the i-CRS parameter R goes to zero. Accordingly, the i-CRS diffraction travel time operator reads as follows:

$$t_D = \frac{1}{V} \sqrt{(x_m - h - x_c)^2 + H^2} + \frac{1}{V} \sqrt{(x_m + h - x_c)^2 + H^2}. \tag{2}$$

We now parametrise Equation 2 in apex coordinates so that the summed amplitudes are assigned to the apex of the diffraction operator. This parametrisation can be achieved by minimising the diffraction travel time
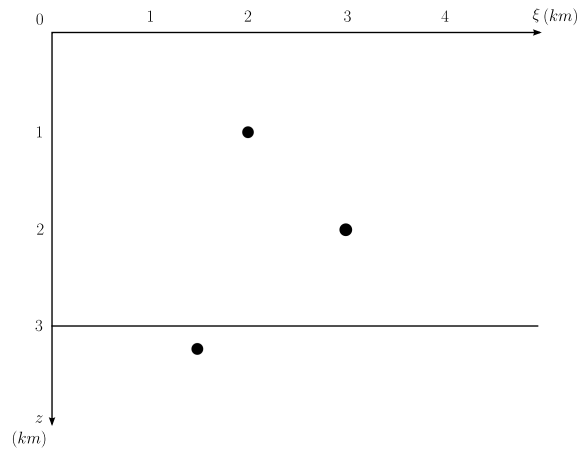
$$\frac{\partial t_D}{\partial x_m} \stackrel{!}{=} 0, \tag{3}$$

with the condition of $h = 0$. The extremum is located at $x_m = x_c$ and $t_D = 2H/V$ with the resulting apex coordinates

$$x_{apex} = x_c \quad , \quad t_{apex} = \frac{2H}{V}. \tag{4}$$

These lead to the i-CRS PreSTM operator in apex coordinates,

$$t = \sqrt{\frac{t_{apex}^2}{4} + \frac{(\Delta x_m - h)^2}{V^2}} + \sqrt{\frac{t_{apex}^2}{4} + \frac{(\Delta x_m + h)^2}{V^2}}, \tag{5}$$

Figure 2: Model geometry: three diffractors and a horizontal reflector are located in a medium with constant velocity.

where $\Delta x_m = x_m - x_{apex}$ is the midpoint displacement. The same result for the poststack case (see Bobsin, 2014) was also derived by Mann (2002).

Equation 5 is a DSR operator that can be used if a suitable velocity is chosen. In order to achieve this, Schwarz (2011) related the i-CRS parameters x_c, H and R to the CRS attributes α, R_{NIP} and R_N. A Taylor series expansion of Equation 1 up to second order and a coefficient comparison with the CRS equation (Müller, 1999) yields

$$V = \frac{v_{NMO}}{\sqrt{1 + \frac{v_{NMO}^2}{v_0^2} \sin^2 \alpha}} \qquad (6a)$$

with

$$v_{NMO} = \sqrt{\frac{2\, v_0\, R_{NIP}}{t_{apex}\, \cos^2 \alpha}}. \qquad (6b)$$

Equations 6 express the migration velocity V that depends on four parameters: the incidence angle α, the radius of curvature of the normal incidence point (NIP) wave front R_{NIP}, a prescribed near-surface velocity v_0, and the considered time t_{apex}. This result for the migration velocity was initially derived and investigated by Bobsin et al. (2013).

In the following section, we first apply the i-CRS stacking and time migration method to simple and complex synthetic data to verify is suitability. A second test on a complex field data set is then performed to investigate the resulting image quality.

APPLICATION

Simple synthetic example

In a first, generic, example we consider a homogeneous model with three diffractors and a reflector (see Figure 2) to apply the i-CRS stacking and PreSTM operator. The data were generated with the Seismic Unix routine `susynlv`. The constant model velocity is 2000 m/s. Offsets and CMP's range from 0–2000 m, and the peak frequency is 30 Hz. Added noise leads to a signal-to-noise ratio of 5.

Figure 3 shows the stacked image (a), the calculated velocity model (b), and the migrated image (c). The apertures used for stacking are $x_m = 500$ m and $h = 2000$ m. The stacked section shows the expected diffraction hyperbolas and the horizontal reflection. The calculated velocity model coincides with the medium velocity. The PreSTM performed with this model and an aperture of 2000 m in midpoint and 1000 m in offset direction collapses the diffractions at their apices except for a cross-like structure around

(a) Stack   **(b)** Velocity model   **(c)** PreSTM
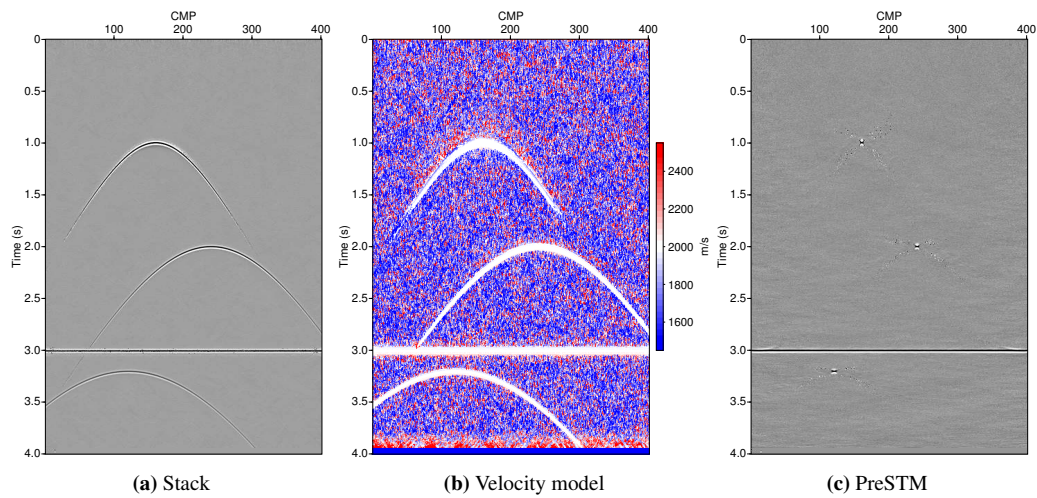
Figure 3: Time imaging results of the generic model.
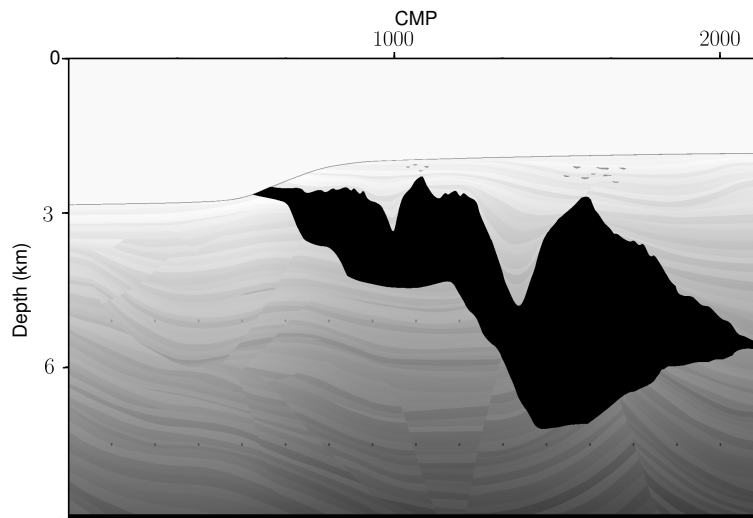
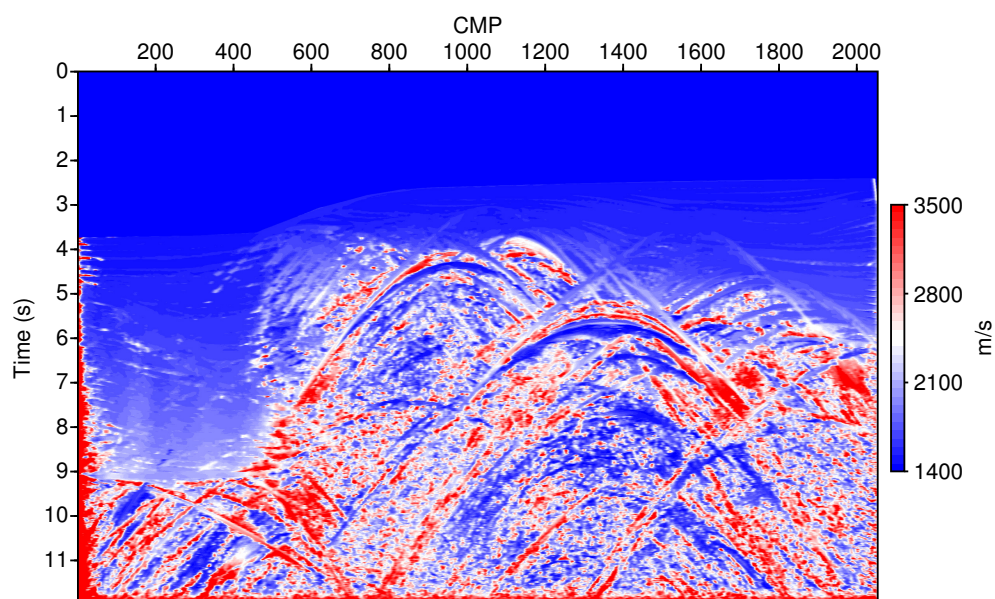**Figure 4:** Stratigraphy of the Sigsbee2A data set.

the apex. This is due to the fact that the range of the first Fresnel zone is infinite for diffractions and thus an infinite aperture is required to image diffractions without artifacts. In reality, however, the aperture is restricted. This issue does not apply to the reflection, which is correctly imaged.

For this simple example, the velocity model and subsurface structure have been reconstructed. In the following section, we investigate the performance of the new method for a complex synthetic data set.

Complex synthetic example

The Sigsbee2A model provided by SMAART JV is a synthetic marine data set that contains a salt body embedded in a sedimentary environment (see Figure 4). In addition, steep faults and two rows of diffractors are incorporated. A lot of these features are difficult to image. Therefore, the Sigsbee2A model often serves as a benchmark model for migration algorithms.

We have stacked and migrated the data. The resulting velocity model is shown in Figure 5. For the sediments on the left, we find the expected slow increase in velocity with depth. Diffraction hyperbolas associated with the rugged top of salt on the right are described by lower velocities than the surrounding

Figure 5: Calculated migration velocity for the Sigsbee2A data set. The high velocities at the edges are caused by boundary effects (see text).

salt.

Figure 6 shows a close-up of the stacked image (a) and the migrated image (b) of the left sedimentary part of the model. To obtain the stacked section we used a midpoint aperture of 300 m at the top and 500 m at the bottom. The offset aperture ranges from 1000 m to 4000 m from top (2 s) to bottom (11 s). To generate the PreSTM we used a midpoint aperture of 2000 m at the top and 4000 m at the bottom. The offset aperture ranges from 1000 m to 5000 m. The stack shows parts of diffraction hyperbolas and indications of faults. Furthermore, a continuous sedimentary layering is visible. The listric fault and its antithetical faults are well defined in the PreSTM. Furthermore, the diffraction hyperbolas are collapsed and the six diffractions in the excerpt are resolved. The left border features smaller amplitudes as well as more noise in the PreSTM section that is not so crisp in these areas. A reason for this is likely to be an incorrect parameter estimation due to less traces at the border, which leads to an incorrect migration velocity.

Figure 7 shows a close-up of the left top of salt area. The rough top of salt results in many diffractions in the stacked image (a). Above the top of salt, sedimentary layering is visible. The resolution of this layering is the same in the PreSTM image (b). Furthermore, the diffractions are collapsed and the top of salt is well resolved. The steeper parts of the syncline are not continuously imaged in the PreSTM. Reasons for this are the acquisition and conflicting dips in the stacked section that lead to an incorrect parameter estimation.

The PreSTM has focused complex features like the rough top of salt and the diffractor rows, which are difficult to recognise in the stacked section. After the successful application of the stacking operator and the PreSTM to synthetic data, we now apply the method to field data.

Field data example

The marine data from the Eastern Mediterranean we investigate in this section were provided by TGS. The acquired seismic line is located in the Levantine basin, which is bounded by the Cyprus arc in the north, the Levantine coast in the east, and the Egyptian coast in the south. The basin is characterised by complex salt tectonic. Figure 8 shows the geological profile of the seismic line. Above the salt rollers (marked orange in the figure), parallel pretectonic units (yellow) are identifiable. They are separated from the syntectonic units (ochre) by a slump complex (grey). The slide of the slump complex could be caused by, e.g., over-steepening or initial salt tectonic.

The velocity model obtained from the stacking is shown in Figure 9. The velocities increase with increasing time until the ocean bottom multiple is reached, starting at 2.4 s TWT at the left. Three to four

(a) Stack
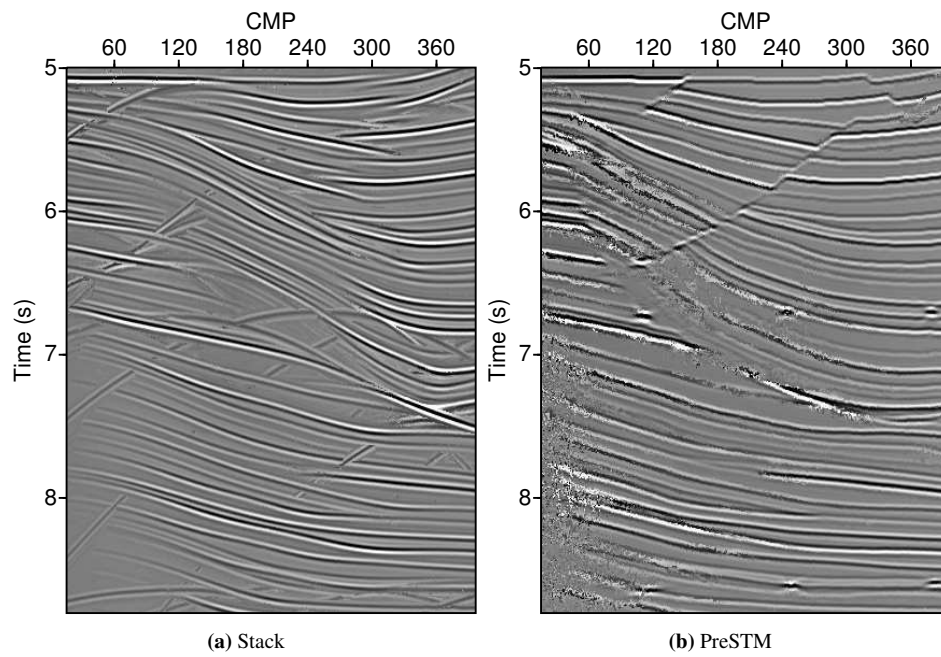
(b) PreSTM

Figure 6: Sigsbee example: close-up shows listric fault and diffractions. Noise in the PreSTM is present where conflicting dips occur and at the border.


(a) Stack

(b) PreSTM
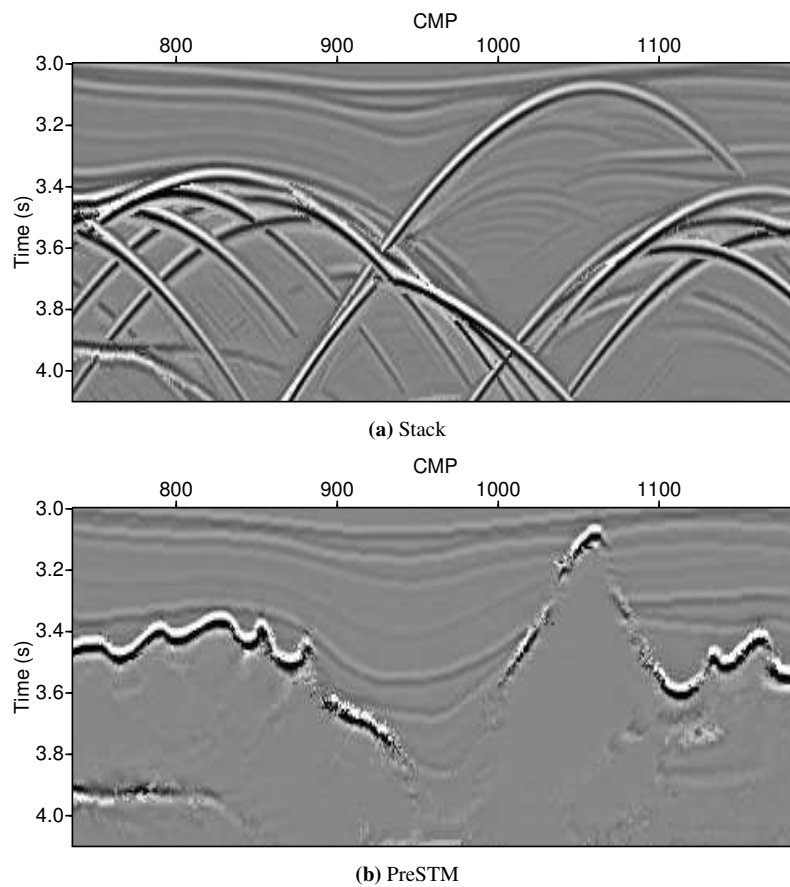
Figure 7: Sigsbee example: close-up showing the top of salt area.
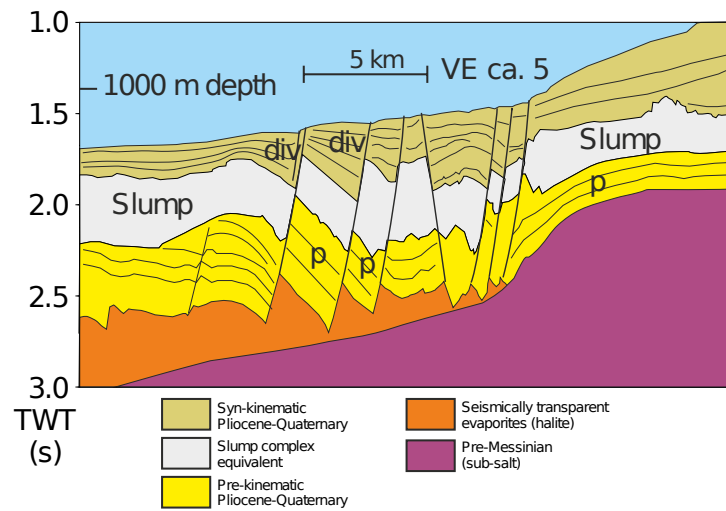
Figure 8: Salt tectonic in the Levantine basin (Hübscher and Netzeband, 2007). Note that this line is striking in the opposite direction of the following seismic sections.
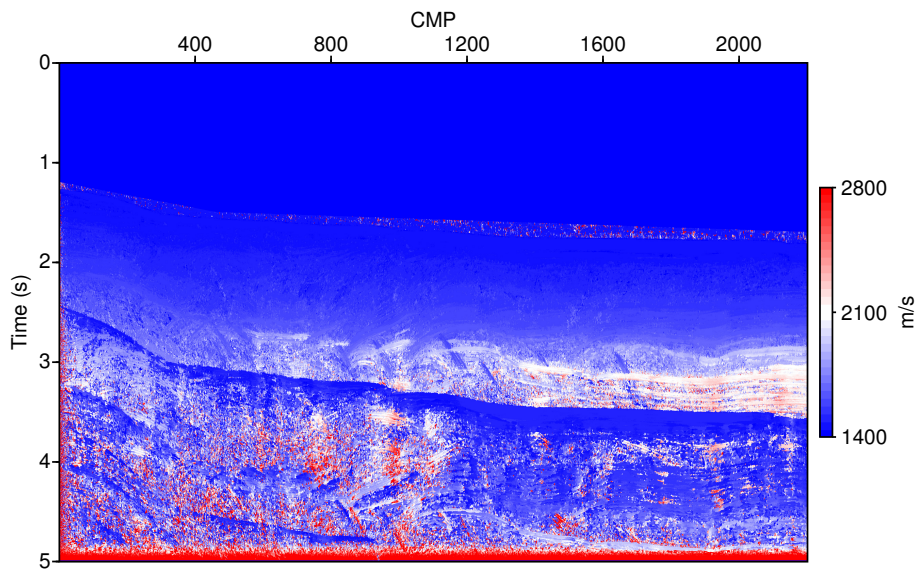
Figure 9: Calculated migration velocity for the field data. The water column is muted and only a small part above the seafloor is visible. Boundary effects lead to the high velocities at the edges.

(a) Stack

(b) PreSTM
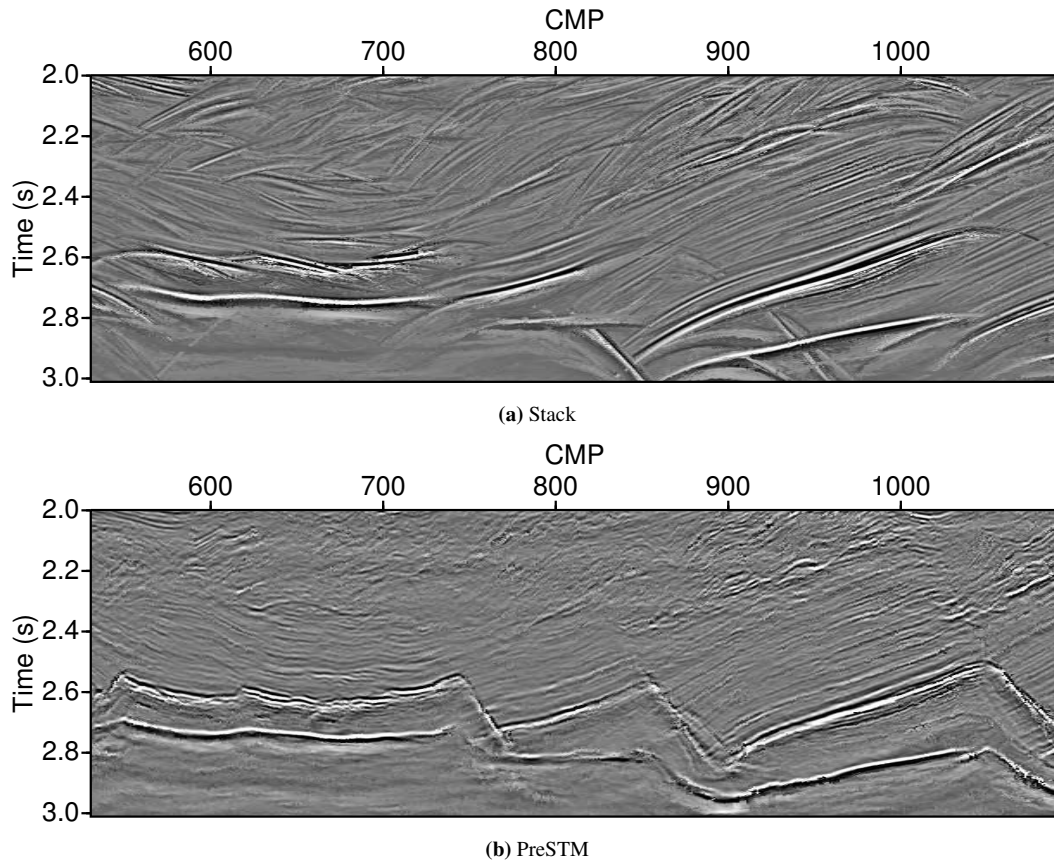
Figure 10: This close-up shows the salt rollers in the field data.

units of the same velocity are identifiable. Starting at the seafloor, these are the syntectonic unit, the slump complex, the pretectonic unit, and the salt unit.

Figure 10 shows a close-up of the data where salt rollers occur. To obtain the stacked section (a), we used a midpoint aperture of 260 m at the top and 1000 m at the bottom. The offset aperture was 2000 m. To generate the PreSTM image (b), we used a midpoint aperture from 1500 m to 2500 m and offsets from 1000 m to 7000 m. The stack shows prominent reflections which indicate the salt body due to higher impedance contrasts. Above the salt, a parallel layering is present. Diffractions are visible in the upper part. The PreSTM resolves the salt rollers with a high definition. Furthermore, a parallel layered pretectonic unit is identified above the salt complex. Although the PreSTM collapses the diffractions, the upper part shows a chaotic pattern due to the predominant geological situation (slided slump complex). Again, we find that our method has lead to a well resolved migrated image.

CONCLUSIONS

In this work, we have introduced a new PreSTM operator based on the i-CRS method. Migration velocities are calculated from two kinematic wave field attributes that are determined from an i-CRS stack, a prescribed near-surface velocity, and the considered time. The PreSTM is therefore a data-driven approach without user interaction. Application to a simple synthetic model showed that the PreSTM is able to migrate diffractions as well as reflections. Examples for more complex synthetic and field data confirm that the subsurface structure and migration velocities can be determined reliably with our new method also for these situations.

Furthermore, additional aspects of the new method, e.g., the influence of the choice of stacking and migration apertures on the resulting image, which are not shown in this paper, were investigated by Bobsin

(2014).

REFERENCES

Bobsin, M. (2014). Time Migration applying the i-CRS Operator. Master's thesis, University of Hamburg.

Bobsin, M., Gajewski, D., Schwarz, B., and Vanelle, C. (2013). A new stacking operator: i-CRS with four parameters. *16th Annual WIT report*, pages 34–44.

Gelchinsky, B., Berkovitch, A., and Keydar, S. (1999). Multifocusing homeomorphic imaging – part 1: Basic concepts and formulae. *Journal of Applied Geophysics*, 42:229–242.

Hubral, P. (1983). Computing true amplitude reflections in a laterally inhomogeneous earth. *Geophysics*, 48:1051–1062.

Hübscher, C. and Netzeband, G. L. (2007). *Evolution of a young salt giant: The example of the Messinian evaporites in the Levantine Basin*, pages 175–184. Taylor & Francis Group. In: The Mechanical Behaviour of Salt – Understanding of THMC Processes in Salt.

Mann, J. (2002). *Extensions and Applications of the Common-Reflection-Surface Stack Method*. PhD thesis, University of Karlsruhe.

Mayne, W. (1962). Common reflection point horizontal data stacking techniques. *Geophysics*, 27:927–938.

Müller, T. (1999). *The Common Reflection Surface stack method – Seismic imaging without explicit knowledge of the velocity model*. PhD thesis, University of Karlsruhe.

Schwarz, B. (2011). A new nonhyperbolic multi-parameter operator. Master's thesis, University of Hamburg.

Schwarz, B., Vanelle, C., Gajewski, D., and Kashtan, B. (2014). Curvatures and inhomogeneities: An improved common-reflection-surface approach. *Geophysics*, 79(5):S231–S240.

Vanelle, C., Kashtan, B., Dell, S., and Gajewski, D. (2010). A new stacking operator for curved subsurface structures. *80th Ann. Internat. Mtg. Soc. Expl. Geophys.*

Yilmaz, O. (2001). *Seismic Data Analysis*. SEG, Tulsa.